Article:
Zhang, H, Li, X, Han, B et al. (2 more authors) (2018) Simultaneous reactive dyeing and surface modification of polyamide fabric with TiO_2 precursor finish using a one-step hydrothermal process. Textile Research Journal, 88 (22). pp. 2611-2623. ISSN 0040-5175

https://doi.org/10.1177/0040517517729382

Simultaneous Reactive Dyeing and Surface Modification of Polyamide Fabric with TiO_2 Precursor Finish using One-Step Hydrothermal Process

Abstract: In this paper, a facile approach of dyeing polyamide (PA) fabric by using C.I. Reactive Blue 19 dye and simultaneously modifying it with titanium dioxide precursor under hydrothermal condition is developed. The anthraquinone-based Reactive Blue 19 dye, which is more resistant to biodegradation owing to its fused aromatic structure compared to azo-based one, is utilized as a model compound in this research to demonstrate the photodegradation effect of TiO_2 on reactive dyes. It is shown that a layer of TiO_2 nanoparticles is homogeneously coated on fiber surfaces and their particle sizes are smaller than those remaining in the residual dyeing liquors. The crystallinity and optical property of the resultant PA fabrics are changed due to this hydrothermal-dyeing process. In comparison with the solely dyed PA fabrics, the PA fabrics dyed and simultaneously modified with anatase TiO_2 nanoparticles exhibit better color fastnesses against artificial light (Xenon) while maintain similar grades of color fastnesses against washing with soap, wet scrubbing, dry cleaning as well as dry/wet rubbing. While changes in the tensile strength, elongation and water absorbency of the resultant PA fabrics were not found, the addition of tetrabutyl titanate in the dyeing liquor is proved to facilitate the reaction of reactive dye with PA fabric and the resultant PA fabric shade. More interestingly, it is noticed that the residual dyeing liquor can be photodegradated after 50 mins of either UV or visible light irradiations, and the dyeing wastewater can thus be released eco-friendly to the environment.

Keywords: Polyamide (PA) fabric; dyeing; surface modification; titanium dioxide,

hydrothermal

1 Introduction

Among a variety of common dyestuffs, reactive dyes have been widely used in the textile industry mainly due to their color stability and brilliant hues.[1] Recent studies have reported that reactive dyes composed of reactive functional groups are highly soluble in water and have a high degree of reactivity with textile fibers by means of covalent bonds,[2] ionic bonds,[3] hydrogen bonds,[4] and van der Waals forces[5] during dyeing process. However, wastewater treatment of effluents from dyeing process is always a key concern for textile industries. The discharge of textile dyehouse effluents into aquatic environment can cause public health and safety concerns. This is because the unexhausted dyes in dyeing wastewater have intensive colors and are generally cytotoxic, mutagenic, and carcinogenic chemicals.[6] Up to now, traditional wastewater treatment techniques such as coagulation, flocculation, filtration, and biodegradation are expensive and ineffective to remove the reactive dyes from textile wastewater.[7-9] Therefore, it is desirable to explore alternative methods for the degradation of reactive dyestuffs in a more effective, environmentally friendly, and sustainable route.

The photocatalytic oxidation degradation of dyeing wastewater has increasingly gained considerable interest because it is more effective and capable of degrading any complex organic chemicals in comparison with other purification methods.[10-12] It has been demonstrated that the photodegradation conditions such as catalyst loading, pH and initial concentration of the dyestuff have a great effects on the decolourization and degradation of textile dyes,[13] while the presence of some dyeing auxiliary chemicals inhibits the photocatalytic decolourization and degradation.[14, 15] Anatase titanium dioxide (TiO_2) has a wide band gap of 3.2 eV and is one of

the most extensively used photocatalyst in the treatment of wastewater containing organic and dye pollutants[16-21] because of its low cost, nontoxicity, physical and chemical stability, and unique electronic and optical properties.[22-25] For instance, the photocatalytic degradation kinetics of reactive dyes including Reactive Red 11, Reactive Red 2, Reactive Orange 84, Reactive Orange 16 and Reactive Black 5 in aqueous suspensions of TiO_2 under visible light have been examined.[26] The photocatalysis mechanism of TiO_2 involves the adsorption of photons, the generation of electron-hole pairs and subsequently the production of reactive hydroxyl radicals ($HO\cdot$) for the completely destroy of pollutants in wastewater.[27]

Textile fibers or fabrics are ideal catalyst substrates for the deposition of TiO_2 particles due to their large specific surface area, high surface characteristics, and good mechanical properties.[28, 29] Many studies have been carried out to modify polyamide (PA) fabrics by either dispersing nano-scaled TiO_2 particles within polymeric matrices or coating TiO_2 on the surface of PA fabrics in order to produce potentially self-cleaning PA fabrics, as well as to improve their strength, wettability, dyeability, and electrical conductivity.[30-34] The influences of TiO_2 quantity on nylon-6 granules and yarns properties has been investigated.[35] Besides, TiO_2 finishing has been applied to cotton,[36] linen,[37] silk,[38] wool,[39] viscose,[40] aramid,[41] polyester,[42] and polyester/wool blended [43] fabrics by pad-dry-cure process to prepare functional textiles. However, very few have been reported on the textile technology to produce the dyed and TiO_2 modified textile fabrics in a single step process.[44, 45]

The aim of this study is to develop a hydrothermal-dyeing process to modify and dye PA fabric using titanium sulfate or tetrabutyl titanate precursor in conjunction with C.I. Reactive Blue 19 dye under hydrothermal conditions. The representative anthraquinone-based Reactive Blue 19 dye is utilized as a model compound because it is more resistant to biodegradation

owing to its fused aromatic structure compared to azo-based one.[46] The residual dyeing liquors were collected and irradiated with UV or visible light. The photoactivities of the remaining particles on the residual dyeing liquor were then estimated by measuring the absorbance of residual dyeing liquor against irradiation time.

The surface morphology, crystalline phase, chemical composition, microstructure, and optical property of the resultant PA fabrics are characterized by using field emission scanning electron microscopy (FE-SEM), X-ray diffraction (XRD), energy dispersive X-ray spectroscopy (EDX), sequential inductively coupled plasma emission spectroscopy (ICPS), transmission electron microscopy (TEM), and diffuse reflectance spectrum (DRS) techniques. The changes of the tensile strength, water absorption capacity, air permeability, and color fastness of the resultant PA fabrics as well as the particle size distributions of TiO_2 particles are also measured. As a comparison, exhaustion of reactive dye and photodegradation of residual dyeing liquor are investigated.

2 Experimental

2.1 Materials

A plain woven fabric made of 100% polyamide (PA, $[NH(CH_2)_5CO]$) filaments was purchased from Haiyan Jiaxia Chemical Fiber Co. Ltd. The linear densities of its warp and weft yarns are 8.3 tex, and the numbers of threads in warp and weft directions are 420 and 300 ends per 10 centimeters respectively. All of the chemicals used in this experiment were of analytical reagent grade, including titanium sulfate ($Ti(SO_4)_2$), urea (NH_2CONH_2), tetrabutyl titanate ($Ti(OC_4H_9)_4$), 25% ammonium hydroxide ($NH_3 \cdot H_2O$), sodium carbonate (Na_2CO_3), glacial acetic acid (CH_3COOH), acetone (CH_3COCH_3), and anhydrous ethanol (CH_3CH_2OH). The C.I.

Reactive Blue 19 dye (CAS No.2580-78-1, $C_{22}H_{16}N_2Na_2O_{11}S_3$) was kindly provided by Baden Aniline and Soda Factory (BASF) (China) Co. Ltd. Shanghai. All solutions were prepared using deionized water.

2.2 One-step Hydrothermal-dyeing Treatment of PA Fabrics

Prior to treatment, about 1.6 g of PA fabrics was cleaned with 100 ml of acetone, anhydrous ethanol, and deionized water at 40^{o}C for 15 min successively.

Two hydrothermal-dyeing treatment schemes were designed for the purpose of comparing the effect of different TiO_2 precursors on fabric dyeing. Two TiO_2 precursors, namely titanium sulfate and tetrabutyl titanate, were used to modify the pretreated PA fabrics respectively. Unlike the previous studies,[47, 48] where tetrabutyl titanate (or titanium sulfate and urea) was solely used in the fabric modifications, the TiO_2 precursor in this study was mixed with the Reactive Blue dye liquor to treat PA fabric under hydrothermal condition. The time duration used for the hydrothermal-dyeing process for the two different TiO_2 precursors were set as 5 and 3 hours respectively based on previous solely hydrothermal experiments[47, 48] in order to produce anatase TiO_2 particles.

Firstly, 0.016 g of C.I. Reactive Blue 19 dye (1% of the weight of fabric (o.w.f)) was completely dissolved in 80 ml deionized water at a liquor ratio of 1:50 under constant stirring, the pH value of this dye bath was then adjusted to 4.5 by adding a certain amount of glacial acetic acid.

In Scheme one, 0.5 g of titanium sulfate was added into the above dye bath under vigorous stirring at room temperature, followed by adding 0.25 g of urea. The pH value of the dyeing liquor decreased from 4.5 to 1.6. The pretreated PA fabric was then immersed in the dyeing liquor for 5 min. The dyeing liquor along with the fabric was immediately transferred to a 100

ml PTFE sealed container which was placed in a stainless steel autoclave. Ultimately, the autoclave was laid in a furnace and run at a rotation rate of 60 revolutions per minute, it was heated to 120°C at a heating rate of 2°C per minute. After 3 h of hydrothermal reaction, the autoclave was cooled naturally down to room temperature. The pH value of the resultant solution was found to be 6.4.

In Scheme two, 0.5 g of tetrabutyl titanate was added into the dye bath under vigorous stirring at ambient temperature. The pH value of the dyeing liquor increased from 4.5 to 6.0 and the hydrothermal reaction time was set at 5 h. The other processing conditions were the same as in the scheme one. The pH value of the resultant solution was found to be 4.0.

In order to compare fabric properties, for example fabric tensile strength, water absorption, air permeability and color fastness, PA fabrics were solely dyed with C.I. Reactive Blue 19 at 120°C for 5 hours without the addition of any TiO_2 precursor. The pH value of the resultant solution was found to be 3.4.

The hydrothermal-dyeing treated PA fabrics were then immersed in an aqueous ammonium hydroxide solution (pH=8.5) at 85°C for 20 min for the purpose of color fixing. They were then soaked with a suspension containing 2 g/L of soap and 2 g/L of sodium carbonate at 95°C at a liquor ratio of 1:30 for 15 min, and subsequently washed with acetone, ethanol and deionized water for 15 min respectively, and finally dried at 80°C. The as-synthesized particles remaining in the suspension were collected by centrifugation and successively washed with acetone, anhydrous ethanol and deionized water respectively, and dried at 120°C. The masses of as-obtained particles were measured by using an analytical balance (Sartorius Cubis MSE125P) for further analyses.

2.3 Characterization and Measurement

Surface morphologies of both PA fabrics and as-synthesized particles were characterized by using Field Emission Scanning Electron Microscope (FE-SEM, Quanta 450 FEG+X-MAX50). The chemical compositions of the PA fabrics from both of the two schemes were determined by Energy Dispersive X-ray Spectroscope (EDX) attached to the FE-SEM instrument.

The crystallinity of both PA fabrics and as-synthesized particles were analyzed using X-ray Diffraction (XRD, Shimadzu 7000S X-ray diffractometer system) and calculated using MDI Jade 5.0 software. The scanning angle 2θ was recorded from 5° to 80° using Cu $K\alpha_1$ radiation (λ=0.1540562 nm) at 40 kV and 40 mA. The crystal sizes of as-synthesized particles were determined using Scherrer equation $D=K\lambda/\beta cos\theta$ (where D was the diameter of the particle, λ was the X-ray wavelength, β was the FWHM of the diffraction line, θ was the diffraction angle, and K was a constant 0.89).[49]

Contents of Ti element on the resultant PA fabrics were identified using a Sequential Inductively Coupled Plasma Emission Spectrometer (ICP2060T, Skyray Instruments), and the microstructures of the cross-section of the resultant PA fibers were investigated by using Transmission Electron Microscope (TEM, JEOL3010, 200 keV).

Particle size distributions of the as-synthesized TiO_2 particles were examined in a Zetasizer Nano ZS90 particle size analyzer (Malvern Instruments Ltd.).

Diffuse Reflectance Spectra (DRS) of the resultant PA fabrics over the range of 200–800 nm were performed in a UV-Visible/NIR spectrophotometer (Hitachi U-3010) with an integration sphere ø150 mm. The fabric specimens were folded so that the light could not transmit through the tested fabrics.

Tensile properties of resultant PA fabrics were measured in a HD 026N electromechanical tester (Nantong Hongda Experiment Instruments Co., Ltd) against standard GB/T3923.1-2013

(or ISO 13934-1:2013). The gauge length was 200 mm and the fabric width was 50 mm. The extension speed was 100 mm/min and the pre-tension was 2 N.

The water absorbency of the PA fabrics were evaluated according to GB/T 23320-2009 (or ISO 18696:2006) and were calculated by equation (1) below.

$$G_w = \frac{(m_w - m_c)}{m_c} \times 100\% \qquad (1)$$

Where G_w was the water absorbency (%), m_w and m_c were the masses (g) of wet and dry PA fabrics respectively.

Air permeabilities of the PA fabrics were assessed against GB/T 5453-1997 (or ISO 9237:1995).

The color depths (*K/S* values) at the maximum absorption wavelength of 592 nm and CIE 1976 (L^*, a^*, b^*) color coordinates of dyed PA fabrics were measured in an X-Rite CA22 spectrophotometer under D65 illuminant and 10^o standard observer. Color fastnesses against washing with soap, wet scrubbing, artificial light (Xenon), dry cleaning, and rubbing were tested according to GB/T 3921-2008 (or ISO 105-C10:2006), GB/T 420-2009 (or ISO 105-C07:1999), GB/T 8427-2008 (or ISO 105-B02:2013), GB/T 5711-2015 (or ISO 105-D01:2010), and GB/T 3920-2008 (or ISO 105-X12:2001), respectively. The changes in color and staining were judged by references set in GB/T 250-2008 (or ISO 105-A02:1993) and GB/T 251-2008 (or ISO 105-A03:1993), respectively. The binding strengths of the synthesized particles onto PA fabrics were examined by FE-SEM.

The dyeing liquors were centrifuged on a TG16-WS high speed centrifuge (Hunan Xiang Yi Laboratory Instrument Development Co., Ltd) at a speed of 12000 r/min for 10 min. Dye exhaustion during dyeing process was then estimated using the UV absorbance of dyeing liquor

at 592 nm in a UV-1600 spectrophotometer (Beijing Rayleigh Analytical Instrument Corp.). The deionized water was used as the reference solution. The dye exhaustion E (%) was calculated by the equation (2) below,[35]

$$E(\%) = \left(1 - A_1 / A_0\right) \times 100\% \qquad (2)$$

Where A_0 was the absorbance of raw dyeing liquor before dyeing fabrics, A_1 was the absorbance of residual dyeing liquor after dyeing fabrics.

Photocatalytic degradation of residual dyeing liquor was conducted on a photochemical reactor (YM-GHX-V, Shanghai Yuming Instrument Co., Ltd) equipped with a 1000 W mercury lamp. About 50 mL of residual dyeing liquor was added into a quartz glass tube under magnetic stirring, and irradiated with UV and visible light irradiations, respectively. For UV light irradiation, the UV-passing filters were used to block off visible light and allow the UV light of 254 nm in wavelength and of 2.35 mW/cm^2 in radiation intensity which was measured in a ST-512 UV illumination meter, to be used for the irradiation. The UV cut-off filters were employed to simulate visible light irradiation and allow visible light of the intensity much greater than 2×10^7 lux measured by a TES 1332A digital light intensity meter, for the irradiation experiment. The absorbance of residual dyeing liquor before and after the irradiation, A_1 and A_2, for a time duration of t (minutes) were measured at 592 nm in the UV-1600 spectrophotometer. The decolorization grade D (%) due to photocatalytic degradation was calculated by the equation (3) below,[11]

$$D = (1 - A_2 / A_1) \times 100\% \qquad (3)$$

Furthermore, the transmission spectra of residual dyeing liquor in the range of 200-800 nm were obtained by using the same spectrophotometer. All above measurements were repeated three times and the average was given.

3 Results and Discussion

3.1 Surface Morphology Observations

The FE-SEM images of surface morphologies of four PA fabrics, including untreated, solely dyed, titanium sulfate (Scheme one) and tetrabutyl titanate (Scheme two) treated PA fabrics are shown in Figure 1. The surface of untreated PA fabrics is relatively smooth without any attachments. Some small particles added in the spinning process are found [Fig. 1(a)]. In comparison with the untreated PA fabric, the surface of the solely dyed PA fabric has no distinct change except a film of organic matters [Fig. 1(b)]. But for both titanium sulfate and tetrabutyl titanate treated PA fabrics, a layer of aggregated substances is coated on their fiber surfaces. From the high resolution FE-SEM images illustrated in the upper left corner, it is found that these tiny clusters are composed of nano and submicrometer sized particles [Fig. 1(c) and 1(d)]. The average size of the particles deposited on the titanium sulfate treated PA fabric is apparently larger than that deposited on the tetrabutyl titanate treated one. However, the morphologies of those particles attached to PA fabrics are similar to the particles formed in hydrothermal process treatment of polyamide fabric without dyeing.[48]

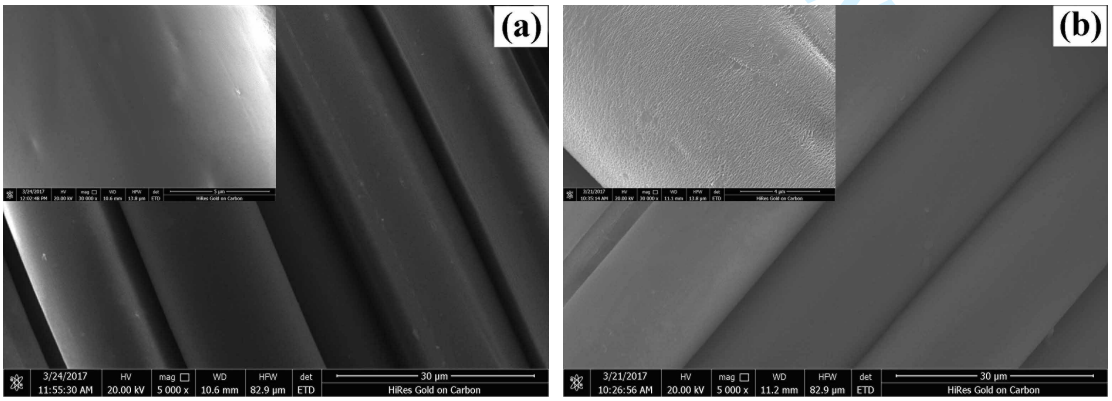

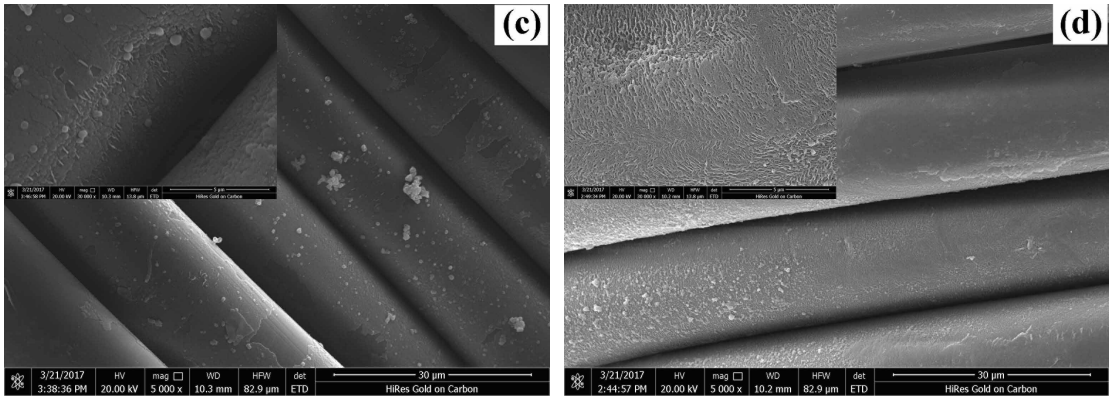

Figure 1. FE-SEM images of PA fabrics: (a) untreated; (b) solely dyed with reactive dye; (c) Scheme one; (d) Scheme two

3.2 Crystalline Phase Analysis

XRD patterns of both PA fabrics and as-synthesized particles are shown in Figure 2. Apparently, the intense diffraction peaks at around 2θ=21.5°, which is ascribed to the reflection of (200)/(001) of the γ crystal form of PA, for the solely dyed, titanium sulfate and tetrabutyl titanate treated PA fabrics are significantly weakened after one-step hydrothermal treatments. Furthermore, the diffraction peaks at about 2θ=20.2° and 23.6°, corresponding to the reflection of (200) and (002)/(202) of the α crystal form of PA, are obviously strengthened. The results indicate that the transformation of meta-stable γ-phase to more stable α-phase[50] occurs during hydrothermal treatment at high temperature and high pressure. The crystallinities of PA fibers increase from 27.8% for untreated PA fabric to 43.8% for fabric solely dyed with Reactive Blue 19. The crystallinities further increase to 45.4% and 46.5% when PA fabrics are treated with titanium sulfate and tetrabutyl titanate in hydrothermal-dyeing processes, respectively. The results suggest that the hydrolysis and recrystallization primarily occur in the amorphous region of PA fiber.[51] However, the diffraction peaks of TiO_2 are not observed in the XRD patterns of PA fabrics treated with titanium sulfate and tetrabutyl titanate precursors. This might be because the amount of TiO_2 particles immobilized on PA fabrics is so small that it can not be detected by

the XRD system. Thus, the crystal structures of as-synthesized TiO_2 particles are characterised. A series of typical peaks centered at 25° (101), 38° (004), 48° (200), 54° (105), 55° (211) and 62° (204) are observed in the XRD patterns of as-synthesized particles, which are in accord with the anatase structure of TiO_2 (JCPDF Card No.21-1272).[52] Based on the width of the peaks at 2θ=25°, 38° and 48° and calculation using the Scherrer's equation, the mean crystallite sizes of as-synthesized particles are found to be 10.1 nm for Scheme one and 10.2 nm for Scheme two.

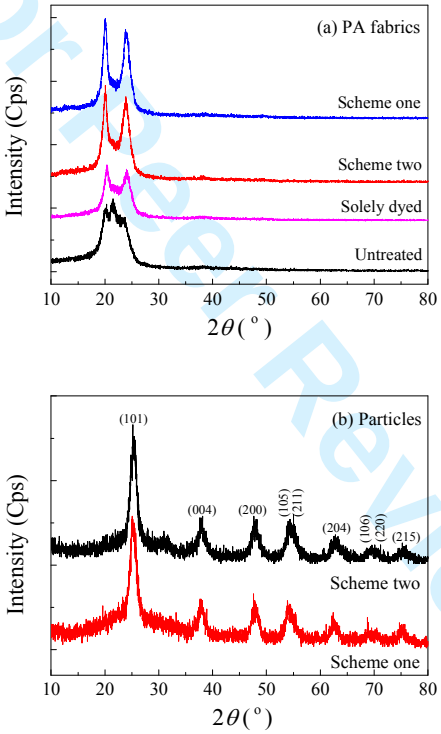

Figure 2. XRD patterns of (a) PA fabrics and (b) as-synthesized particles

3.3 Cross-section of PA Fibers Deposited with TiO_2 Particles

TEM and high-resolution images, and selected area electron diffraction (SAED) patterns of the cross-sections of PA fibers having TiO_2 particles deposited on the fabric surfaces are shown in Figure 3. It is noted that a thin layer of TiO_2 particles is uniformly coated on the surface of PA fibers treated with titanium sulfate and tetrabutyl titanate precursors, respectively. The

thicknesses of the aggregates of nano-scaled TiO_2 particles deposited on the fiber surface are about 200 nm for both schemes, and hardly any TiO_2 particle is distributed beneath the PA fiber surface. From the high-resolution TEM images, the particle size of the TiO_2 particles obtained from both of the schemes is around 10 nm. The distances between adjacent lattice planes are found to be 0.354 nm and 0.356 nm for the schemes one and two respectively, which are very close to the d-spacing 0.35 nm of the (101) plane of anatase TiO_2. The corresponding SAED patterns of TiO_2 particles indicate that the TiO_2 nanoparticles are crystalline for both schemes. Moreover, the diffraction rings in the corresponding electron diffraction patterns are assigned to the lattice planes (101), (004), (200), (105) and (211) of anatase TiO_2.

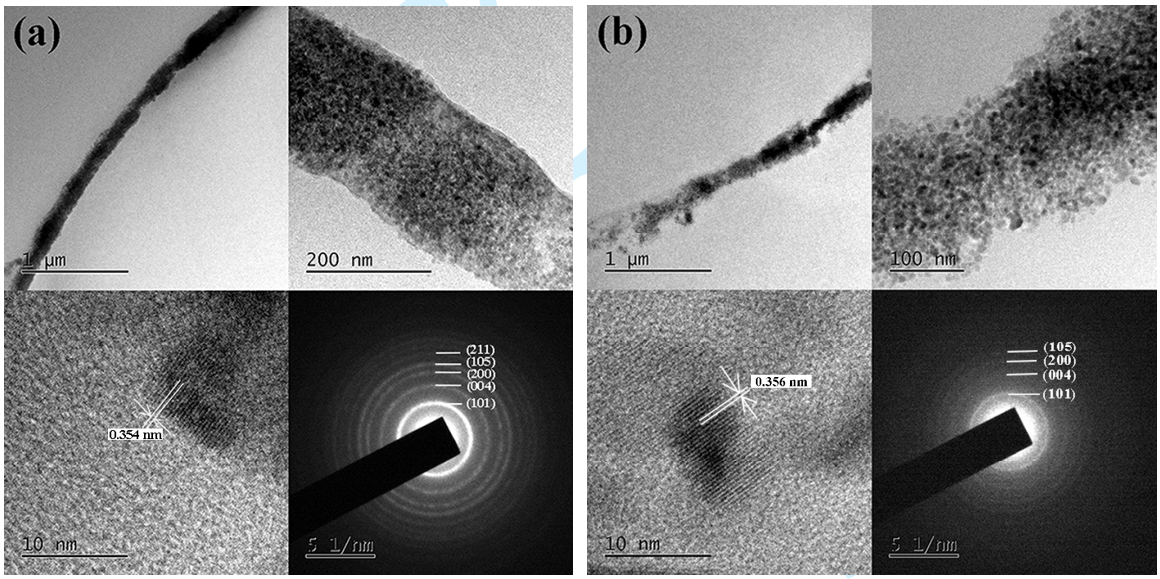

Figure 3. TEM and high-resolution TEM images, and SAED patterns for PA fibers obtained in (a) Scheme one and (b) Scheme two

3.4 Particle Sizes of the Remaining TiO_2 Particles

Particle size distributions of the remaining TiO_2 particles in residual solutions for both schemes measured using the particle size analyzer (ZS90, Malvern Instruments Ltd.) as well as their FE-SEM images are shown in Figure 4. It is noticed in the FE-SEM images that all of the

particles are aggregated together. The TiO_2 particle aggregates produced in Scheme one are in the range of 1100 nm to 2350 nm in dimensions, they are slightly larger than those (in the range of 800 nm to 1500 nm) produced in Scheme two. The coagulation of the submicrometer and micrometer sized TiO_2 particles might be mainly caused by reactive dye and dyeing agents. Besides, the size and surface topography of TiO_2 particles have a considerable influence on their extent of aggregation. It is common for individual nanoparticles to aggregate together as clusters due to both their large surface area and great van der Wales attraction forces between them. Additionally, it is noticed that the TiO_2 particle aggregates coated on PA fibers are significantly smaller than those remaining in the residual dyeing liquors. This may be because the growth of TiO_2 nanoparticles on PA fibers is somehow restricted by the matrix of polyamide polymers.

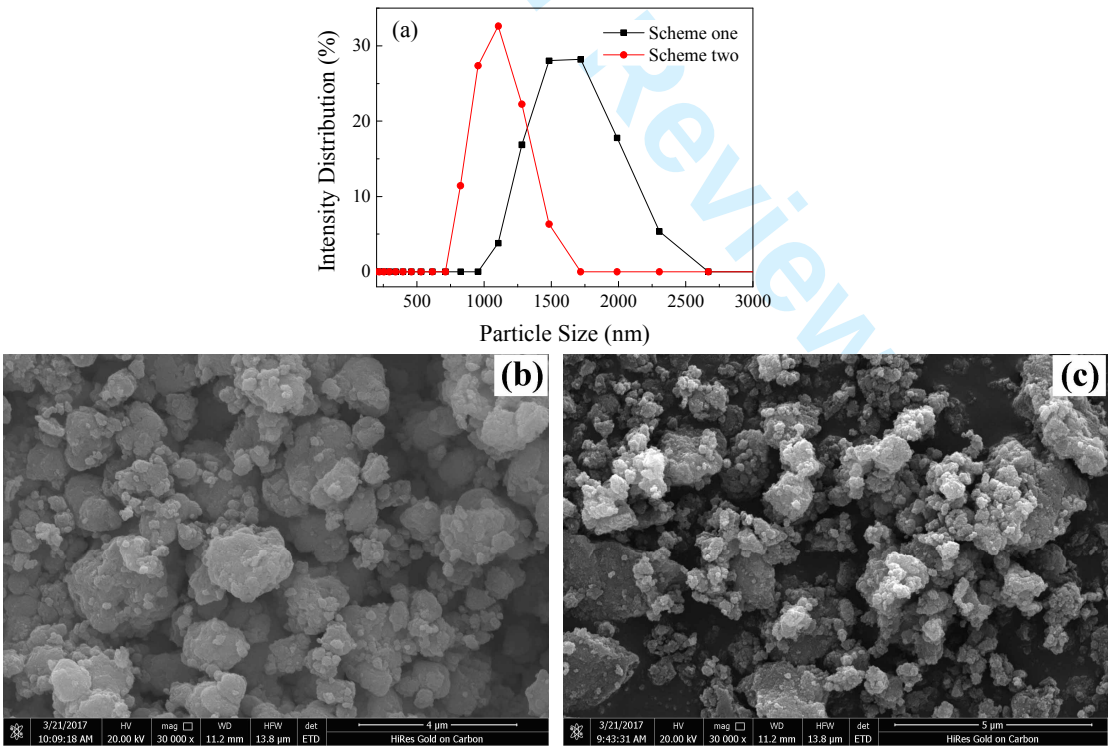

Figure 4. Particle size distribution (a) and FE-SEM images of TiO_2 particles for (b) Scheme one and (c) Scheme two

3.5 Optical Property Analysis

DRS of the untreated, solely dyed, titanium sulfate and tetrabutyl titanate treated PA fabrics are shown in Figure 5. The optical images of dyed PA fabrics are inserted in Figure 5. It is clear that the untreated PA fabric has a great capability of absorbing UV light in the range of wavelengths smaller than 350 nm. There are two characteristic absorption peaks at 230 nm and 320 nm, which are attributed to the electronic $\pi \rightarrow \pi^*$ transitions of the carbonyl amide group and benzene of PA, respectively.[53] When PA fabrics are solely dyed with C.I. Reactive Blue 19, a characteristic absorption band at around 310 nm is ascribed to the chromophore components of the dye molecules,[46] and another broad absorption band is observed primarily in the wavelength range of 550–650 nm, confirming the conjugated system of C.I. Reactive Blue 19 dye with anthraquinone structure.[6] The DRS of the titanium sulfate and tetrabutyl titanate treated PA fabrics are greatly influenced by the dye used which has an intense absorption peak in the visible light region. At the same time, they are also influenced by the coating of TiO_2 nanoparticles on fabric surface, which is caused by the electron promotion of TiO_2 from the valence band to the conduction band.[10] In comparison with the untreated PA fabric, more than 22.5% and 10.2% of UV lights for the titanium sulfate treated PA fabric are absorbed in UVA and UVB wavebands respectively, while more than 35.3% and 13.2% of UV lights for the tetrabutyl titanate treated PA fabric can be absorbed in UVA and UVB wavebands, respectively. The average reflectance for Scheme one is much greater than that for Scheme two, indicating the color of the tetrabutyl titanate treated PA fabric is darker than that of the titanium sulfate treated one. This has been confirmed by the optical images.

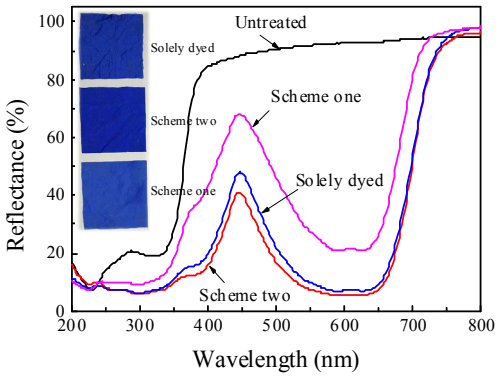

Figure 5. Diffuse reflectance spectra of PA fabrics

3.6 Tensile Properties

The changes of fabric structural parameters and tensile properties of the untreated, solely dyed, titanium sulfate and tetrabutyl titanate treated PA fabrics are shown in Table 1. It is found that the numbers of yarns in both warp and weft directions of the PA fabrics increase slightly which indicates the occurence of fabric shrinkages during dyeing and hydrothermal processes. The fabric shrinkage seems intensified due to the interactions between titanium precursor and PA fabrics,[48] as the presence of TiO_2 nanoparticles on the surface of PA fibers leads to greater surface roughness in PA yarns. During the fabric stretching process, the friction resistance between PA yarns or fibers would increase in comparison with the smooth PA fibers without TiO_2 particles deposited on their surfaces. Therefore, the greater tensile strengths and elongations at break of the fabrics from both of the schemes are due to both the presence of titanium particles in the fabrics and the shrinkages of the PA fabrics in both directions during hydrothermal-dyeing treatment.

Table 1. The results of fabric structural changes and tensile properties of PA fabrics (standard deviations are in parentheses)

PA fabric	Number of yarn picks (ends/10cm)	Tensile strength (N)	Elongation (%)

	Warp	Weft	Warp	Weft	Warp	Weft
Untreated	420	300	629.0 (±12.6)	474.0 (±11.2)	21.8 (±0.8)	23.4 (±1.1)
Solely dyed	425	303	635.7 (±11.8)	482.4 (±11.1)	22.4 (±0.7)	24.1 (±0.9)
Scheme one	445	315	681.0 (±13.7)	518.0 (±12.3)	24.6 (±1.0)	25.2 (±0.8)
Scheme two	448	317	687.0 (±12.5)	525.0 (±12.0)	25.7 (±0.9)	26.1 (±1.0)

3.7 Air Permeability and Water Absorbency

The results of air permeability and water absorbency of PA fabrics are shown in Table 2. Due to the significant shrinkages of PA fabrics in both warp and weft directions after dyeing or hydrothermal-dyeing processes, the fabric air permeabilities decrease sharply from 329.9 mm/s for untreated PA fabrics to 168.3 mm/s for solely dyed PA fabrics, 148.9 mm/s for fabrics from Scheme one and 125.8 mm/s for fabrics from Scheme two. This indicates smaller fabric porosities after dyeing and hydrothermal-dyeing processes.

The water absorbency of the untreated PA fabric is 14.2%, while after hydrothermal treatments, the water absorbencies of the treated fabrics are 15.8% for the solely dyed PA fabrics, 16.7% for fabrics from Scheme one and 16.5% for fabrics from Scheme two. With consideration of the decrease of the fabric porosities, the increased fabric absorbency might be due to the improved fabric wettability owing to both the interaction of the water molecules with the hydrophilic TiO_2 particles coated on fabric surface and the increased fiber surface roughness. [54, 55]

Table 2. The results of air permeability and water absorbency of PA fabrics

PA fabric	Air permeability (mm/s)	Water absorbency (%)
Untreated	329.9	14.2
Solely dyed	168.3	15.8
Scheme one	148.9	16.7
Scheme two	125.8	16.5

3.8 Color Fastnesses

The *K/S* values, CEI $L^*a^*b^*$ color coordinates, and ratings of color fastness for the treated PA

fabrics are shown in Table 3. Interestingly, the *K/S* value of the solely dyed PA fabric is much greater than that of the titanium sulfate treated PA fabric (Scheme one) but smaller than that of the tetrabutyl titanate treated PA fabric (Scheme two). The existence of tetrabutyl titanate in dyeing liquor is known to make the reactive dye molecules diffuse more easily into PA fibers[56] probably due to its neutral pH and special affinity to dyes. The color fastnesses against artificial light (Xenon) for the fabrics from both of the schemes are grade 6, which is better than the grade 5 for the solely dyed PA fabric, mainly ascribing to the coating of TiO_2 particles on the fabric surfaces. The color fastnesses against washing with soap, wet scrubbing, dry washing, dry and wet rubbing are grade 5 for the solely dyed, titanium sulfate and tetrabutyl titanate treated PA fabrics. The results indicate the reactive dyes can penetrate into the matrix of PA fibers. It is demonstrated by FE-SEM observation that the fiber surfaces of PA fabrics treated in both schemes are still coated with some of the aggregated particles even after being wet scrubbed for 20 cycles, suggesting strong binding forces between the PA fibers and TiO_2 particles.[57, 58] It is found in EDX element analysis that, on the fabrics after 20 cycles of wet scrubbing, the atom percentages of Ti element decrease from 1.49% to 0.74% for the titanium sulfate treated PA fabric and from 1.44% to 0.44% for the tetrabutyl titanate treated PA fabric, respectively. Moreover, the results of ICP emission spectrometry indicate that the atomic masses of Ti element decrease from 920.41 μg/g to 653.54μg/g for Scheme one and from 367.98 μg/g to 284.4 μg/g for Scheme two, respectively. The reductions of Ti element for both schemes are caused by the losses of TiO_2 particles attached to the surfaces of PET fabrics during the process of being wet scrubbed for 20 cycles.

Table 3. *K/S* values, CIE $L^*a^*b^*$ coordinates and color fastnesses of dye PA fabrics

PA fabric	*K/S*	CIE $L^*a^*b^*$	Rating of color fastness

	value	L^*	a^*	b^*	Washing	Wet scrubbing	Light: Xenon	Dry cleaning	Rubbing	
									Dry	Wet
Solely dyed	8.47	38.75	6.82	-41.03	5	5	5	5	5	5
Scheme one	4.83	46.48	5.04	-40.94	5	5	6	5	5	5
Scheme two	11.16	36.17	10.94	-45.13	5	5	6	5	5	5

3.9 Dye Exhaustion in Hydrothermal-dyeing Process

It is known that tetrabutyl titanate belongs to an organometallic chemical compound with colorless or pale-yellow color. It can decompose in water solution at near neutral pH to form TiO_2 particles, which are deposited on the surface of PA fabrics during hydrothermal-dyeing process. As a result, there is no considerable change in the dye exhaustion of PA fabric treated with tetrabutyl titanate. On the contrary, titanium sulfate is an inorganic chemical compound with strong acidity and affects the dyeing behavior of reactive dyes with PA fabrics. When PA fabric is solely dyed with C.I. Reactive Blue 19 dye, the dye exhaustion is 98.5%, implying almost all dye molecules can be absorbed by the PA fabric under hydrothermal condition. When a TiO_2 precursor is added into the dyeing liquor under hydrothermal conditions, the dye exhaustions are 92.8% and 98.4% for Scheme one and Scheme two respectively. Thus the deposition of TiO_2 particles on fabric surface using titanium sulfate has influences on the affinity of reactive dyes for PA matrix.

The transmission spectra along with optical photographs of residual dyeing liquors are shown in Figure 6. It is evident that the transmission spectra of raw dyeing liquors are well corresponded to the diffuse reflectance spectra of dyed PA fabrics. The characteristic absorption peaks at about 250, 310 and 345 nm in UV region are ascribed to the chromophore components of anthraquinone dye molecules. The major absorption peak at 592 nm in visible light region corresponds to the blue color.[46] The residual dyeing liquor of the solely dyed PA fabric is basically colorless, while the residual dyeing liquors of both hydrothermal schemes are the

solutions of turbid mixtures. The mass percentage concentrations of TiO_2 particles remaining in the residual dyeing liquors are calculated as 0.183 g/L for Scheme one and 0.146 g/L for Scheme two, respectively. As is shown in the optical photographs (see Fig. 6b), the residual dyeing liquor for Scheme two is transparent color and for Scheme one is light blue color after centrifugation. The residual liquors for both titanium sulfate and tetrabutyl titanate precursors without addition of dye and auxiliaries are colorless (not given).

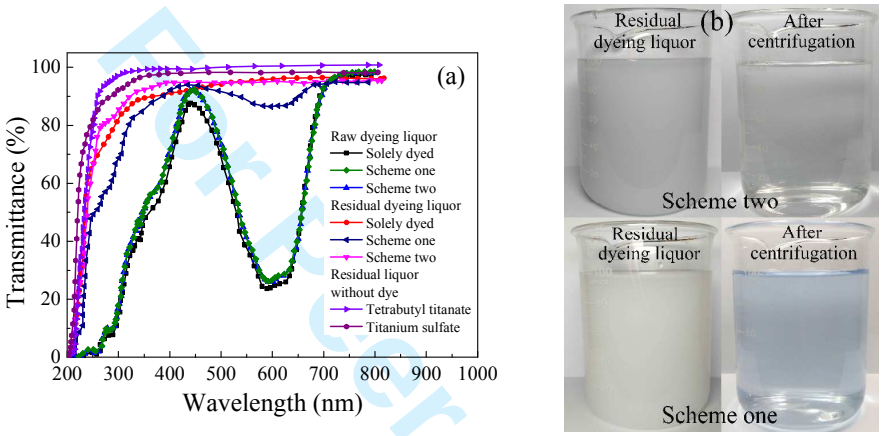

Figure 6. Transmission spectra (a) and optical photographs (b) of dyeing liquors

3.10 Photodegradation of Residual Dyeing Liquor in Scheme One

When the residual dyeing liquors for Scheme one are irradiated with UV and visible lights respectively, the decolorization grades against the increases of irradiation time are shown in Figure 7. It is manifest that the residual dyeing liquors without TiO_2 particles for Scheme one can not be photodegraded under both UV and visible light irradiations. The decolorization grades of residual dyeing liquors with TiO_2 particles gradually increase with the increases of time under both UV and visible light irradiations. There might be two photodegradation mechanisms of C.I. Reactive Blue 19 dye,[59] (1) 'direct' degradation on TiO_2 surface which is more preferentially in acidic and neutral conditions, and (2) 'indirect' degradation mediated by photogenerated OH·which is more rapidly at high pH values. As the irradiation time increases,

some large molecules like Uniblue A sodium salt, sodium naphthalene sulfonate, and vinylsulfonyl aniline gradually break down to the smaller intermediates.[59] The rate of photodegradation under UV light irradiation is greater than that under visible light irradiation. This is because visible light has less quantum energy than UV rays. After 50 mins of irradiation, the decolorization grades are beyond 95% under both UV and visible light irradiations. The transmission spectra of residual dyeing liquors after exposure to UV and visible light irradiations are shown in Figure 8. The characteristic absorption peaks of dye molecules greatly decease after exposure to UV light for 20 min or visible light for 30 min, this implies that the dye molecules in the residual dyeing liquors are almost completely photodegradated to smaller fragments.[60] As a result, the practical application of TiO_2 precursor in dyeing wastewater treatment process for the color removal in dyeing liquors of reactive dyes is of great significance.

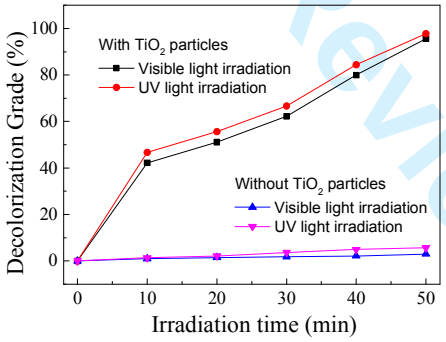

Figure 7. The dynamic decolorization grade of residual dyeing liquors for Scheme one

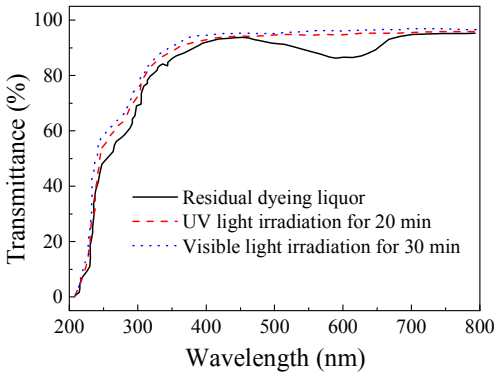

Figure 8. Transmission spectra of residual dyeing liquors for Scheme one before and after exposure to UV and visible light irradiations

Conclusions

In this study, one-step hydrothermal-dyeing process was employed to modify PA fabrics using titanium precursors (either titanium sulfate or tetrabutyl titanate) and dye the fabrics simultaneously with C.I. Reactive Blue 19 dyes. It was found that a layer of TiO_2 nanoparticles is homogeneously coated on fiber surfaces, and the mean particle size of the TiO_2 anchored on fiber surfaces by using titanium sulfate is larger than that by using tetrabutyl titanate. However, their particle sizes are smaller than those remaining in the residual dyeing liquors.

In comparison with the solely dyed PA fabrics, the PA fabrics dyed and simultaneously modified with anatase TiO_2 nanoparticles have different crystallinity and optical property due to the TiO_2 nanoparticles deposited on the surface of their constituent fibres. They also exhibit better color fastnesses against artificial light (Xenon) while maintain similar grades of color fastnesses against washing with soap, wet scrubbing, dry cleaning as well as dry/wet rubbing. However, significant changes in the tensile strength, elongation and water absorbency of the resultant PA fabrics were not found.

It was interesting to note that the addition of tetrabutyl titanate in the dyeing liquor is proved to facilitate the reaction of reactive dye with PA fabric and the resultant PA fabric shade. On the contrary, the addition of titanium sulfate in the dyeing liquor would have deleterious effects on the dyeing process and the resultant PA fabric shade. Further research on such phenomena is ongoing. It was also found that the photocatalytic degradation of residual dyeing liquor could be over 95% after 50 minutes of irradiation exposure to UV or visible light due to the as-synthesized anatase TiO_2 particles remained in residual dyeing liquors.

Acknowledgments:

The authors acknowledge the supports from science and technology program (No. 2015049) of China National Textile and Apparel Council, the Sanqin Scholar Foundation (2017) and Handred Talent Programme of Shaanxi Province, and the China Scholarship Council.

References

1. Parvinzadeh M, Assefipour R and Kiumarsi A. Biohydrolysis of nylon 6,6 fiber with different proteolytic enzymes. *Polym Degrad Stabil* 2009; 94(8): 1197–1205.
2. Bergamini RBM, Azevedo EB and de Araujo LRR. Heterogeneous photocatalytic degradation of reactive dyes in aqueous TiO_2 suspensions: Decolorization kinetics. *Chem Eng J* 2009; 149(1–3): 215–220.
3. Allan GG, Miller ML and Reif WM. Bonding in paper and nonwovens. *Text Res J* 1972; 42(11): 675–681.
4. Suganea A, Watanabea A, Okadaa Y and Moritab Z. The stability of monochlorotriazinyl reactive dyes on cellulose films in aqueous alkaline solutions containing peroxide bleaching

agents. *Dyes Pigments* 2001; 50(3): 223–241.

5. Vanja K. Interactions between polysaccharide polymer thickener and bifunctional bireactive dye in the presence of nonionic surfactants. Part 2. Investigation of interactions using SEC method. *Carbohyd Polym* 2002; 50(3): 237–247.
6. Tehrani-Bagha AR, Mahmoodi NM and Menger FM. Degradation of a persistent organic dye from colored textile wastewater by ozonation. *Desalination* 2010; 260(1–3): 34–38.
7. Verma AK, Dash RR and Bhunia P. A review on chemical coagulation/flocculation technologies for removal of colour from textile wastewaters. *J Environ Manage* 2012; 93(1): 154–168.
8. Chong MN, Jin B, Chow CWK and Saint C. Recent developments in photocatalytic water treatment technology: A review. *Water Res* 2010; 44(10): 2997–3027.
9. Saratale RG, Saratale GD, Chang JS and Govindwar SP. Bacterial decolorization and degradation of azo dyes: A review. *J Taiwan Inst Chem E* 2011; 42(1): 138–157.
10. Xu YJ, Zhuang YB and Fu XZ. New insight for enhanced photocatalytic activity of TiO_2 by doping carbon nanotubes: A case study on degradation of benzene and methyl orange. *J Phys Chem C* 2010; 114(6): 2669–2676.
11. Duta A and Visa M. Simultaneous removal of two industrial dyes by adsorption and photocatalysis on a fly-ash–TiO_2 composite. *J Photoch Photobio A* 2015; 306: 21–30.
12. Visa M, Isac L and Duta A. New fly ash TiO_2 composite for the sustainable treatment of waste water with complex pollutants load. *Appl Surf Sci* 2015; 339(1): 62–68.
13. Muruganandham M and Swaminathan M. Solar photocatalytic degradation of a reactive azo dye in TiO_2-suspension. *Sol Energ Mat Sol C* 2004; 81(4): 439–457.
14. Madhu GM, Raj LAMA and Pai KVK. Titamium oxide (TiO_2) assisted photocatalytic

degradation of methylene blue. *J Environ Biol* 2009; 30(2): 259–264.

15. Visa M, Andronic L and Duta A. Fly ash-TiO_2 nanocomposite material for multi-pollutants wastewater treatment. *J Environ Manage* 2015; 150: 336–343.

16. Barakat MA. Adsorption and photodegradation of Procion yellow H-EXL dye in textile wastewater over TiO_2 suspension. *J Hydro-environ Res* 2011; 5(2): 137–142.

17. Bansal P and Sud D. Photodegradation of commercial dye, Procion Blue HERD from real textile wastewater using nanocatalysts. *Desalination* 2011; 267(2–3): 244–249.

18. Kuo CY, Pai CY, He CC, Un CJ and Cheng CM. Photodegradation of aqueous reactive dye using TiO_2/zeolite admixtures in a continuous flow reactor. *Water Sci Technol* 2012; 65(11): 1963–1969.

19. Bansal P and Sud D. Photocatalytic degradation of commercial dye, CI Reactive Red 35 in aqueous suspension: Degradation pathway and identification of intermediates by LC/MS. *J Mol Catal A-Chem* 2013; s374–375: 66–72.

20. Daels N, Radoicic M, Radetic M, Van Hulle SWH and De Clerck K. Functionalisation of electrospun polymer nanofibre membranes with TiO_2 nanoparticles in view of dissolved organic matter photodegradation. *Sep Purif Technol* 2014; 133: 282–290.

21. Saud PS, Pant B, Park M, Chae SH, Park SJ, EI-Newehy M, Al-Deyab SS and Kim HY. Preparation and photocatalytic activity of fly ash incorporated TiO_2 nanofibers for effective removal of organic pollutants. *Ceram Int* 2015; 41(1): 1771–1777.

22. Mahmoodi NM, Arami M, Limaee NY, Gharanjig K and Ardejani FD. Decolorization and mineralization of textile dyes at solution bulk by heterogeneous nanophotocatalysis using immobilized nanoparticles of titanium dioxide. *Colloid Surfaces A* 2006; 290(1–3): 125–131.

23. Chekir N, Benhabiles O, Tassalit D, Laoufi NA and Bentahar F. Photocatalytic degradation

of methylene blue in aqueous suspensions using TiO_2 and ZnO. *Desalin Water Treat* 2015; 57(13): 1–7.

24. Banerjee S, Dionysiou DD and Pillai SC. Self-cleaning applications of TiO_2 by photo-induced hydrophilicity and photocatalysis. *Appl Catal B-Environ* 2015; s176–177: 396–428.

25. Ge MZ, Cao CY, Huang JY, Li SH, Chen Z, Zhang KQ, Al-Deyab SS and Lai YK. A review of one-dimensional TiO_2 nanostructured materials for environmental and energy applications. *J Mater Chem A* 2016; 4(18): 6772–6801.

26. Chatterjee D, Patnam VR, Sikdar A, Joshi P, Misra R and Rao NN. Kinetics of the decoloration of reactive dyes over visible light-irradiated TiO_2 semiconductor photocatalyst. *J Hazard Mater* 2008; 156(1–3): 435–441.

27. Soutsas K, Karayannis V, Poulios I, Riga A, Ntampegliotis K, Spiliotis X and Papapolymerou G. Decolorization and degradation of reactive azo dyes via heterogeneous photocatalytic processes. *Desalination* 2010; 250(250): 345–350.

28. Lombardi M, Palmero P, Sangermano M and Varesano A. Electrospun polyamide-6 membranes containing titanium dioxide as photocatalyst. *Polym Int* 2011; 60(2): 234–239.

29. Vaez M, Moghaddam AZ, Mahmoodi NM and Alijani S. Decolorization and degradation of acid dye with immobilized titania nanoparticles. *Process Saf Environ* 2012; 90(1): 56–64.

30. Zohoori S, Yazdanshenas ME and Davodiroknabadi A. Production of polyamide 6 filled with nano TiO: Effect of temperature, strength and dyeing. *Asian J Chem* 2012; 24(4): 1541–1546.

31. Zohoori S, Karimi L and Ayaziyazdi S. A novel durable photoactive nylon fabric using electrospun nanofibers containing nanophotocatalysts. *J Ind Eng Chem* 2014; 20(5):

2934–2938.

32. Peyravi M, Jahanshahi M, Rahimpour A, Javadi A and Hajavi S. Novel thin film nanocomposite membranes incorporated with functionalized TiO_2 nanoparticles for organic solvent nanofiltration. *Chem Eng J* 2014; 241(241): 155–166.

33. Cossich E, Bergamasco R, de Amorim MTP, Martins PM, Marques J, Tavares CJ, Lanceros-Mendez S, and Sencadas V. Development of electrospun photocatalytic TiO_2-polyamide-12 nanocomposites. *Mater Chem Phys* 2015; 164: 91–97.

34. Abdal-hay A, Mousa HM, Khan A, Vanegas P and Lim JH. TiO_2 nanorods coated onto nylon 6 nanofibers using hydrothermal treatment with improved mechanical properties. *Colloid Surface A* 2014; 457: 275–281.

35. Tayebi HA, Yazdanshenas ME, Rashidi AS, Khajavi R and Montazer M. Effect of delustering agent on physical and mechanical properties of nylon 6. *Asian J Chem* 2011; 23(1): 398–402.

36. Dong YC, Bai ZP, Zhang LW, Liu RH and Zhu T. Finishing of cotton fabrics with aqueous nano-titanium dioxide dispersion and the decomposition of gaseous ammonia by ultraviolet irradiation. *J Appl Polym Sci* 2006; 99(1): 286–291.

37. Ibrahim NA, Eid BM, Hashem MM, Refai R and El-Hossamy M. Smart options for functional finishing of linen-containing fabrics. *J Ind Text* 2010; 39(3): 233–265.

38. Zheng CH, Qi ZM, Shen WC and Chen GQ. Self-cleaning *Bombyx mori* silk: room-temperature preparation of anatase nano-TiO_2 by the sol–gel method and its application. *Color Technol* 2014; 130(4): 280–287.

39. Behzadnia A, Montazer M, Rashidi A and Mahmoudi RM. Rapid sonosynthesis of N-doped nano TiO_2 on wool fabric at low temperature: introducing self-cleaning, hydrophilicity,

antibacterial/antifungal properties with low alkali solubility, yellowness and cytotoxicity. *Photochem Photobiol* 2014; 90(6): 1224–1233.

40. Fahmy HM, Eid RAA, Hashem SS and Amr A. Enhancing some functional properties of viscose fabric. *Carbohyd polym* 2013; 92(2): 1539–1545.

41. Deng H and Zhang HD. In situ synthesis and hydrothermal crystallization of nanoanatase TiO_2–SiO_2 coating on aramid fabric (HTiSiAF) for UV protection. *Microsc Res Techniq* 2015; 78(10): 918–925.

42. Allahyarzadeh V, Montazer M, Nejad NH and Samadi N. In situ synthesis of nano silver on polyester using NaOH/Nano TiO_2. *J Appl Polym Sci* 2013; 129(2): 892–900.

43. Haji A, Shoushtari AM, Mazaheri F and Tabatabaeyan SE. RSM optimized self-cleaning nano-finishing on polyester/wool fabric pretreated with oxygen plasma. *J Text I* 2016; 107(8): 985–994.

44. Alebeid OK and Zhao T. Simultaneous dyeing and functional finishing of cotton fabric using reactive dyes doped with TiO_2 nano-sol. *J Text I* 2016; 107(5): 625–635.

45. Hezavehi E, Shahidi S and Zolgharnein P. Effect of dyeing on wrinkle properties of cotton cross-linked by butane tetracarboxylic acid (BTCA) in presence of titanium dioxide (TiO_2) nanoparticles. *Autex Res J* 2015; 15(2): 104–111.

46. Fanchiang JM and Tseng DH. Degradation of anthraquinone dye C.I. Reactive Blue 19 in aqueous solution by ozonation. *Chemosphere* 2009; 77(2): 214–221.

47. Yang L and Zhang H. Modification of polyamide fabric using tetrabutyl titanate by low temperature hydrothermal method. *J Text Res* 2011; 32(11): 83–89.

48. Zhang H and Yang L. Immobilization of nanoparticle titanium dioxide membrane on polyamide fabric by low temperature hydrothermal method. *Thin Solid Films* 2012; 520(18):

5922–5927.

49. Robert K, Marta S and Imre D. Photooxidation of dichloroacetic acid controlled by pH-stat technique using TiO_2/layer silicate nanocomposites. *Appl Catal B-Environ* 2006; 68(1–2): 49–58.

50. Shi K, Ye L and Li GX. Structure and hydrothermal stability of highly oriented polyamide 6 produced by solid hot stretching. *RSC Adv* 2015; 5(38): 30160–30169.

51. Rangari D and Vasanthan N. Study of strain-induced crystallization and enzymatic degradation of drawn poly(L-lactic acid) (PLLA) films. *Macromolecules* 2012; 45(18): 7397–7403.

52. Zhan HQ, Yang XF, Wang CM, Liang CL and Wu MM. Multiple growth stages and their kinetic models of anatase nanoparticles under hydrothermal conditions. *J Phys Chem C* 2010; 114(34): 14461–14466.

53. Shi KH, Ye L and Li GX. In situ stabilization of polyamide 6 with reactive antioxidant. *J Therm Anal Calorim* 2015; 119(3): 1747–1757.

54. Li Y and Joo CW. Pore structure and liquid behavior of nonwovens composed of nanosized fibers by conjugate spinning. *J Appl Polym Sci* 2012; 126(S2): E252–E259.

55. Hashemizad S, Montazer M and Rashidi A. Influence of the surface hydrolysis on the functionality of poly(ethylene terephthalate) fabric treated with nanotitanium dioxide. *J Appl Polym Sci* 2012; 125(2): 1176–1184.

56. Adeel S, Usman M, Haider W, Saeed M, Muneer M and Ali M. Dyeing of gamma irradiated cotton using Direct Yellow 12 and Direct Yellow 27: improvement in colour strength and fastness properties. *Cellulose* 2015; 22(3): 2095–2105.

57. Han BB, Zhang H, Xu J, Zhang JL Su L. The effect of chitosan on nanometer TiO_2 modified

nylon fabric. *J Xi'an Polytech Univ* 2016; 30(2): 143–149.

58. Zhang H and Zhu H. Preparation of Fe-doped TiO_2 nanoparticles immobilized on polyamide fabric. *Appl Surf Sci* 2012; 258(24): 10034–10041.

59. Abu Bakar F, Ruzicka JY, Nuramdhani I, Williamson BE, Holzenkaempfer M and Golovko VB. Investigation of the photodegradation of Reactive Blue 19 on P-25 titanium dioxide: Effect of experimental parameters. *Aust J Chem* 2015; 68(3): 471–480.

60. He ZQ, Lin LL, Song S, Xia M, Xu LJ, Ying HP and Chen JM. Mineralization of CI Reactive Blue 19 by ozonation combined with sonolysis: Performance optimization and degradation mechanism. *Sep Purif Technol* 2008; 62(2): 376–381.